Radical Polymerization in Homogenized Butyl Acrylate Emulsion

Viera Juraničová, Ignác Capek*

Polymer Institute, Slovak Academy of Sciences, 842 36 Bratislava, Slovakia

Summary: The addition of a small amount of monomer strongly decreased the clouding temperature of nonionic emulsifier (Tween 20). The clouding temperature of the Tween 20 aqueous solution was independent of emulsifier concentration but it strongly varied in the presence of monomer. The decreased cloud temperature was attributed to the penetration of monomer molecules into the interfacial layer that increased the flocculation of microdroplets (monomer-swollen micelles). The surface tension of homogenized ((mini)emulsion) butyl acrylate aqueous emulsion was much smaller than that estimated at or above CMC of Tween 20. The polymerization rate vs. conversion curve of the (mini)emulsion deviates from the three rate intervals typical for the emulsion polymerisation. The shape of the rate-conversion curve reminds more the four rate intervals curve. Interval 2 is overlapped with the initial maximal rate and rate shoulder at higher conversion. The initial maximal polymerization rate ($R_{p,max,1}$) is attributed to the abrupt increase in polymer particles, the polymerization under monomer saturated condition and emulsifier containing peroxide groups ($Tw_{peroxid}$ 20). The rate of emulsion polymerization of BA initiated by ammonium peroxodisulphate (APS) is ca. by one order of magnitude larger than that of blank polymerization (without APS). The second maximal rate (rate shoulder) can result from the gel effect. The more pronounced increase in $R_{p,max,1}$ with Tw 20 concentration supports the presence of peroxide groups. The slight dependence of $R_{p,max,2}$ on [Tw 20] for both APS and DBP (dibenzoyl peroxide) is discussed in terms of the depressed radical entry rate into the close packed surface later of polymer particles. The low activation energy is attributed to the decreased barrier for entering radicals into the polymer particles with increasing temperature. This is more pronounced with the accumulation of covalently bound emulsifier moieties (resulting from $Tw_{peroxid}$ 20) at the particle surface. The ratio of the final number of polymer particles to the initial number of monomer droplets (N_p/N_{drop}) promotes the partial monomer droplet nucleation. The dye approach indicates that the degree of depletion of monomer droplets decreases from the classical emulsion polymerization to the polymerization in pre-homogenized emulsions and the emulsion polymerization with a prolonged-emulsification interval.

Introduction

The increased temperature or addition of a salting-out type electrolyte initiates a dehydration of nonionic emulsifier and its transfer to the oil phase. This is accompanied by the transfer of water from the interface to the bulk. Upon rising the temperature, the nonionic emulsifier micellar phase separates into a dilute phase and a concentrated phase. The cloud curve is a characteristic of such binary water- nonionic emulsifier solutions [1)] and is

 CCC 1022-1360/00/$ 17.50+.50/0

attributed to a dehydration of the polar head of the emulsifier as the temperature increases [2]. Addition of additives (electrolytes) to aqueous solutions of ethoxylated emulsifiers can led to: 1) the decrease of clouding (cloud point – CP) due to a dehydration of the emulsifier by the additive (salt) (salting-out) or 2) the increase of CP reflecting enhanced solubility of the emulsifier in water (salting-in). The structure – making ions (Na, K) lower the hydration of emulsifier polar heads. On the contrary, other ions can be effective in destructuring water and so in the increased solubilization of emulsifier polar heads (salting-in). Some metal ions (Zn^{2+}) salt-in emulsifier by forming complexes with the ether oxygens of polyoxyethylene (PEO) chain [3]. The authors [4] showed that the relevant parameter which controls CP shifts is the ionic surface charge density. The CP variation is related to the changes in micelle-solvent interactions caused by additives.

The binary water-nonionic emulsifier solutions separate into two phases when the temperature is increased above the CP temperature. This temperature is characteristic of the emulsifier and is modified by the addition of a solute. In the same way, the solubilization of organic compounds has been studied in terms of CP variation [5,6]. The direction of the shift of the CP temperature has been interpreted as variations in the overall attractive interaction between the nonionic micelles [7]. For example, CP slightly decreased from 80 to 75 °C with increasing the weight percentage of nonionic emulsifier $\{C_8(EO)_6\}$ from 1 to ca. 10 wt% [8]. The CP temperature (CPT) was decreased by 17 °C when the water/$\{C_8(EO)_6\}$ is saturated with hexachlorocyclohexane (HCH). Furthermore, CP decreased linearly with increasing the mole ratio CHC/emulsifier (λ), for instance, CP decreased from 75 to 60 °C by increased λ from 0.01 to ca. 0.1. The depression of CPT is due to the increasing attraction between micelles (aggregates) [6] . The hydrophobic HCH is assumed to be located in the polar layer of micelles and induces an attraction potential between micelles roughly proportional to the molar ratio HCH/emulsifier.

The high temperature - sensitivity of emulsion stabilized by nonionic emulsifier arises from the high oil-solubility of nonionic emulsifier and the large number of emulsifier molecules adsorbed at the droplet surface and the decrease of HLB, CMC and mean surface area of nonionic emulsifier adsorbed at the interface with temperature [9,10]. The accumulation of nonionic emulsifier in the oil phase at high temperature initiates the formation of inverse micelles (water pools) in the monomer. This is related with the depressed monomer droplet degradation that decreases the amount of monomer and emulsifier in the aqueous phase for

the generation and stabilization of polymer particles. Furthermore, the increased accumulation of polymer in the monomer droplets increases the monomer droplets stability and so droplet nucleation. For example, the presence of predissolved polystyrene (hydrophobe) (ca. 0.5wt %) in the monomer phase increased the stability of monomer droplets (reduced monomer droplet aggregation or Ostwald ripening) [11,12].

The conformation of PEO chains of nonionic emulsifier at high coverage (emulsifier concentration) is extended, making a packing monolayer, impeding EO-surface interactions. At low coverage (low emulsifier concentration), when the flexibility of the EO chains is high, these contacts may occur [13]. A direct consequence of the decreased emulsifier concentration or increased temperature will be the change in the emulsifier layer configuration, which passes from extended to flat and so vary the latex particle stability. The colloidal stability of monomer droplets stabilized by nonionic emulsifier (PEO type) is influenced by the interparticle interaction via the extended surface PEO chains (bridging flocculation mechanism) [14]. The extended degree of PEO chains decreases with increasing temperature and droplet (particle) flocculation in the oil-in-water emulsions is often observed below the CP of emulsifier [15]. The hydrophobicity of the interfacial emulsifier film increases with temperature due to dehydration of the PEO chain [16].

The major thrust of this work is to study the phase behavior of the ternary monomer/Tween 20/water solutions and its relation to the kinetics of emulsion polymerization of homogenized butyl acrylate/Tween 20/water emulsions. We simulate the diffusion-controlled emulsion polymerization of butyl acrylate by increased uniformity and stability of monomer droplets. The effect of the oil-solubility of nonionic emulsifier (HLB), the thickness of interfacial layer and the phase variation on the polymerisation are followed. Furthermore, the kinetics and colloidal parameters of the emulsion polymerization of butyl acrylate stabilized by Tween 20 as a function of reaction conditions, the type of initiator and temperature have been investigated.

Experimental section

Materials. Commercially available butyl acrylate (BA) and styrene (St) (Fluka) were purified by distillation under reduced pressure. Extra pure ammonium peroxodisulfate (APS, Fluka) and dibenzoyl peroxide (DBP, Fluka) were used as supplied. The emulsifiers used were the reagent-grade Tween 20 (Tw 20, non-ionic emulsifier, polyoxyethylene sorbitan monolaurate,

provided by Serva in the form of a 97% aqueous solution) and SDS (sodium dodecyl sulfate). Doubly distilled water was used as a polymerization medium.

Recipe and Procedures. Batch polymerizations of homogenized monomer emulsions ((mini)emulsion) were carried out at different temperatures {50, 60, 70, and 80 °C} with the recipe comprising 100 g water and 40 g BA (or St). The homogenized monomer emulsions were prepared with the homogenizer Ultra Turrax, IKA Works, USA. The amounts of emulsifier (Tw 20) and initiator (APS and DBP) varied as shown later.

The monomer conversion was determined by both the dilatometric and gravimetric methods. The particle size was determined by the light scattering method. The polymerization technique, the preparation of polymer latex for size measurements, the estimation of particle number and particle size distribution were the same as described earlier [17-20].

The coarse emulsion was prepared by dissolving emulsifier (Tw 20 or SDS) and monomer (BA or St) (40 g) in water (100 g) and mixed with a mechanical agitator at 400 rpm for 20 min at room temperature. The resultant coarse emulsion was then homogenized by the homogenizer for 5 min. The average monomer droplet size of diluted (mini)emulsion was followed by the dynamic light scattering method as a function of aging time.

The surface tension determination. The surface tension was determined by the stalagmometric method [21]. A glass-jacketed stalagmometer with a watch glass was used. Constant temperature (25 °C) was maintained by connection of the jacketed stalagmometer to an adjustable temperature water-bath pump.

Monomer-droplet depletion measurements. To determine the degree of consumption of monomer droplets during the polymerization, the emulsion polymerization with the blue dye (0.1 wt% based on monomer) was carried out at 60 °C. The polymer latexes with a different content of polymer were prepared. The latex products were allowed to stand at room temperature over 3 days before UV absorbance measurements. In this manner, a thin layer of blue precipitate can be found on the bottom of the sample. The upper fraction of the latex sample was dissolved in toluene for determination of the blue dye content according the calibration curve.

Cloud-point measurements. The aqueous Tw 20 solutions and the mixtures of Tw 20, monomer (1.3 g St or BA) and water (100 g) were prepared in flasks, stirred for 1 h, and then placed in a circular at 25 °C. The temperature of the circulator was increased 0.2 °C each time until equilibrium was achieved. Each time, the transparency (turbidity) of the emulsifier

solution was checked. Once the turbidity of solution was slightly increased, the temperature was determined to be the CP of the emulsifier solution. The amounts of emulsifier varied as shown later.

Results and Discussion

Cloud point (CP)

The micellar solutions ([Tween 20 (Tw 20)] = 0.04 mol.dm^{-3}) clouded at ca. 55 °C, declouded at ca. 60 °C, and clouded again above 75 °C. The premicellar structures assembled at 55 °C were thermally destabilized, partly destroyed or more packed at 60 °C. At higher [Tw 20] (0.08 mol.dm^{-3} and 0.12 mol.dm^{-3}), the micellar solutions clouded above ca. 77 °C and 79 °C, respectively. At [Tw 20] ≤ 0.04 mol.dm^{-3}, however, declouding at ca. 55 °C was observed. Turbidity at declouding (55 °C) decreased with increasing emulsifier concentration and solutions became transparent at [Tw 20] = 0.08 mol.dm^{-3}. At higher Tw 20 concentrations, the micellar solutions first clouded above ca. 75-77 °C. These data indicate that the destabilization effect is inversely proportional to the emulsifier concentration. The thermal stability of (pre)micellar aggregates increased at high emulsifier concentration and so clouding or additional (supramicellar) aggregation appeared first above ca. 75 °C. At low Tw 20 concentration, the loosely packed emulsifier molecules are thermally instable. On the contrary, the thermally stable close-packed structures (at high emulsifier concentration) are less sensible to changes in temperature. Temporary reversals in particle growth, termed declouding, have been reported during heating episodes in certain nonionic emulsifiers [22].

The temperature at which clouding of the emulsifier solution occurred is nearly independent of Tw 20 concentration (Fig. 1). The cloud point (CP) ca. 80 °C results from the hydrophilic nature of Tw 20 (HLB = 16.7). For a given emulsifier mole fraction, upon rising the temperature, the micellar phase separates into a dilute phase and a concentrated one. The cloud curve of a binary water/Tw 20 solution (Fig. 1) [22] is attributed to a dehydration of the polar head of the emulsifier with temperature [23]. CP of more hydrophilic emulsifier NP40 (the analytical grade, HLB = 17.8), however, was reported to be ca. 80 °C [25]. The increased CP of more hydrophobic Tw 20 (HLB = 16.7) can be attributed to the penetration of byproducts in the emulsifier palisade layer and so the salting-in effect. Indeed, the CMC of the Tw 20 aqueous solution (8 x 10^{-5} mol.dm^{-1}, this work) was larger than that (5 x 10^{-5} mol.dm^{-1}) reported in [26].

The cloud curve of the ternary monomer/Tw 20/water system shows that clouding temperature strongly decreased by the addition of monomer and then increased with increasing emulsifier concentration ([Tw 20]/[Monomer] ratio) and the increase was more pronounced with BA (Fig. 1). The addition of a small amount of solute (BA or St) strongly decreased clouding. The sharp decrease in CP results from the deep penetration of oil into the emulsifier aggregates and to tendency to form an oil pool (swelling). The surfactant layer curvature becomes negative when CP decreases by the addition of solute.

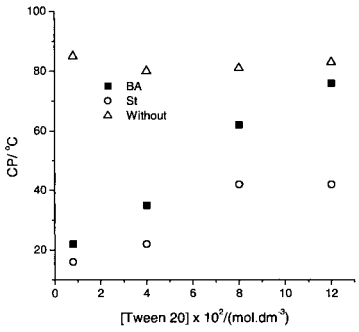

Fig. 1. Variation of clouding (CP/ °C) with Tween 20 concentration and additive type (BA or St). Recipe: 100 g water and 1.3 g BA or St.

The similar behavior (salting-out effect) was observed with sodium acetate [27]. In the same way, the solubilization of organic compounds has been studied in terms of CP variation [5,6]. The direction of the shift of the CP temperature has been interpreted as variations in the overall attractive interaction between the nonionic micelles [28]. For example, CP slightly decreased from 80 to 75 °C with increasing the weight percentage of nonionic emulsifier $\{C_8(EO)_6\}$ from 1 to ca. 10 wt% [8]. The CP temperature decreased by 17 °C when the water/C_8EO_6 solution was saturated with hexachlorocyclohexane (HCH). The hydrophobic solute (St, BA, etc.) is assumed to penetrate the polar layer of micelles and so induce an attraction potential between micelles which is roughly proportional to the molar ratio solute/emulsifier. St is supposed to dehydrate stronger PEO chains and dissolves a larger amount of emulsifier than BA. The less hydrophobic BA (acts as a coemulsifier [29]) can accumulate more in the interfacial layer. This can lead to the hydrogen bonding between polar groups of emulsifier, monomer and water and the "limited salting-in" effect. A salting-out type monomer (BA or St) initiates a dehydration of nonionic emulsifier and its transfer to the oil phase. The extent of transfer increases with temperature and the transfer is more pronounced with a more hydrophobic St. This is connected with the decreased amount of

micellar emulsifier in the aqueous phase. Furthermore, if a molecular volume of oil is large (BA), the clouding curve shifts to higher temperature. This fact means that an emulsifier becomes more soluble in the water phase.

Monomer emulsions and polymer latexes

The surface tension γ of the aqueous Tw 20 solution at and the CMC of Tw 20 (8×10^{-5} $mol.dm^{-1}$ [this work] or 5×10^{-5} $mol.dm^{-1}$ [26]) is in the range 46-48 $mN.m^{-1}$. The further increase of Tw 20 concentration slightly decreased the surface tension. The addition of monomer slightly varied the surface tension of aqueous micellar solution of Tw 20 (1 mM):

$\gamma(mN.m^{-1})$/[BA](mM): 45 /0, 45.5/ 1.3, 45.4/3.5, 45.3/7 Transparent solutions

$\gamma(mN.m^{-1})$/[St](mM): 45 /0, 46.8/ 1.7, 51.4/4.1, 51.4/8.3 Milky solutions

The surface tension slightly increases with increasing St concentration but it is nearly independent of BA. If the monomer molecules are attractively adsorbed at the interface just like emulsifier, the surface tension should decrease. The data show that the BA molecules could concentrate on the micelle surface as a coemulsifier. The increased surface tension could mean the penetration of St molecules into the interfacial layer and then the expulsion of the emulsifier molecules from the interfacial layer. The decreased amount of free amount of emulsifier with increasing amount of monomer is not ruled out. The surface tensions of the homogenized BA/Tw 20/water emulsions ((mini)emulsions), however, are much below 40 $mN.m^{-1}$ or much below the γ_{CMC} value (γ at CMC). The surface tension of water (or hydrogen bonded liquids) is higher than that of apolar liquid such as a pure hydrocarbon. For example, surface tension of water is 72.8 $mN.m^{-1}$, benzene 29 $mN.m^{-1}$, n-octane 21.8 $mN.m^{-1}$, propionic acid 26.7 $mN.m^{-1}$ (at ca. 20 °C), etc. [30,31]. Furthermore, the interfacial tension of BA-water is 30-31 $mN.m^{-1}$ and St-water 40-43 $mN.m^{-1}$, respectively [32]. Tables 1, 2 and 3 show that the surface tension of BA (mini)emulsions are much closer to that of BA-water or the oil (BA). The monomer droplet degradation saturates the aqueous phase around the droplets with monomer and so forms the monomer film around drop.

Table 1 shows that the surface tension increased with conversion (the amount of hydrophobic polymer). Higher hydrophobicity related with lower solubility of monomer in water leads to an increase in the surface tension [33]. The decreased amount of free monomer in the aqueous micellar solution decreases the monomer film formation around drops. The

monomer/polymer particles are expected to act as a swelling agent and so decrease the concentration of monomer within the aqueous micellar solution. The effect of polymers on γ can also be discussed in terms of general monomer/polymer systems taking into account the emulsifier-monomer-polymer interactions [34]. The monomer-polymer interfacial tension is expected to increase with increasing conversion (polymer). The surface tension of poly(butyl acrylate) (PBA) is higher than that of BA. The accumulation of polymer in the monomer phase and the decreased monomer droplet volume, on the contrary, can release emulsifier into the aqueous phase and decrease the surface tension.

Table 1. Variation of colloidal parameters of (mini)emulsion polymerization of BA with conversion.[a)]

Conv. (%)	γ [1)] ($mN\ m^{-1}$)	Conv. (%)	γ [2)] ($mN\ m^{-1}$)	Temp. (°C)	γ [3)] ($mN\ m^{-1}$) b)	c)
0	32	0	32	25	32	
6	36	11	37	30	33.1	
15	40	22	41	40	33.5	
25	42	41	45	50		
37	43	58	45	60		
59	44	72	46			
76	46	87	47			

a) 100 g water, 40 g BA, 60 °C, [Tw 20] = 1.47 x 10^{-2} $mol.dm^{-3}$, [APS] = [DBP] = 1 x 10^{-3} $mol.dm^{-3}$, 60 °C, 1) APS, 2) DBP, $CMC_{Tw20,25\ ^{\circ}C}$ = 8 x 10^{-5} $mol.dm^{-1}$, $\gamma_{CMC,Tw20}$ = 54 dyne cm^{-1}.

A water-insoluble blue dye was used to study the fate of monomer droplets in the classical emulsion, (mini)emulsion and classical miniemulsion polymerisations. Fig. 2 shows the variation of blue dye content (BD/wt%) in the latex product with conversion and polymerisation type. The BD/wt% data were highly scattered up to ca 20% conversion probably due to the phase separation (the appearance of monomer phase on the top of sample). In the classical emulsion polymerisation (CE) the monomer droplets deplete ca. at 50-55% conversion. This is a somewhat larger value than that obtained with static and dynamic swelling methods where the styrene monomer droplets depleted ca. at 40% conversion [35]. The continuous depletion of monomer droplets in the CE polymerization should be paralleled with the release of dye and its precipitation. The shift in the monomer droplet depletion from 40% (a swelling method) to ca. 50% (a dye method) probably results

from the increased stability of monomer droplets caused by the presence of hydrophobe (blue dye) and/or the lower sensitivity of a dye method. In the classical miniemulsion

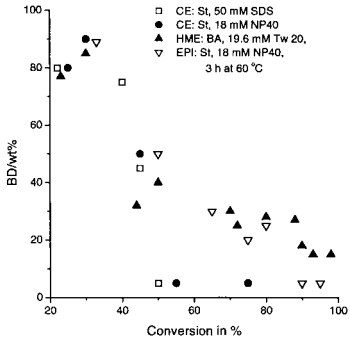

Fig. 2. Variation of blue dye amount in the disperse systems in the classical emulsion (CE) stabilized by with SDS and NP40), (mini)emulsion (HME) stabilized by Tw 20 and emulsion polymerization with prolonged-emulsification interval (EPI) (3 h at 60 °C).

Polymerisation of styrene, the blue dye distributes between the unnucleated monomer minidroplets and the formed monomer/polymer particles [36,37]. The continuous droplet nucleation transforms the medium of dye from monomer to polymer without releasing of dye from the droplets to the aqueous phase. The sample of final polymer latex contains the amount of dye initially charged in the monomer phase. In the emulsion polymerisation with the prolonged-emulsification time (EPI), the monomer droplets are preserved up to the high conversion. This can be attributed to the increased stability of monomer droplets due to the

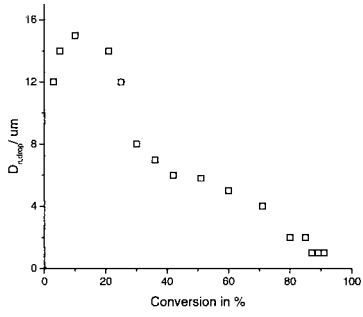

Fig. 3. Variation of number average droplet size ($D_{n,drop}/\mu m$) with conversion in the St emulsion polymerization stabilized by NP40 or NP40/SDS [38].

accumulation of polymer in the monomer phase. The latex samples prepared by the emulsion polymerisation with the prolonged-emulsification time monitored by a video-enhanced microscope preserved the monomer droplets up to ca. 95% conversion (Fig. 3) [38]. In (mini)emulsion polymerisation (HME) of BA, the monomer droplets were preserved up to the final conversion and the final polymer particles contained a small amount of dye. This can be

discussed in terms of the partial nucleation of monomer droplets and/or the agglomeration of polymer particles with the dye-saturated monomer droplets.

Rate of polymerization

The conversion-time data for the polymerization of the coarse BA emulsion and homogenized ((mini)emulsion) BA emulsion initiated by APS or DBP are shown in Figs. 4 and 5. These data show the effect of nonionic emulsifier (Tw 20) concentration on conversion or the rate of polymerization. The emulsifier concentrations were varied in the range from 4.9 x 10^{-3} to 2 x 10^{-2} mol.dm^{-3} much above the CMC of Tw 20 (8 x 10^{-5} mol.dm^{-3}). The conversion curves for emulsion polymerization are concave upward early on with a short linear portion. The linear portion one is more pronounced in the runs with APS. The polymerisation was very slow at high conversion especially with DBP.

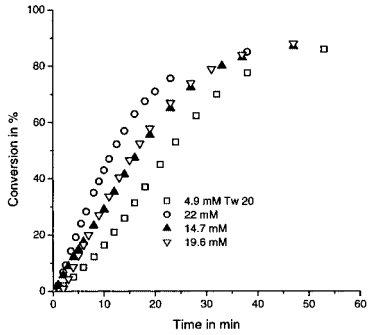

Fig. 4. Variation of monomer conversion with the reaction time and Tw 20 concentration in the (mini)emulsion polymerization of BA initiated by APS.
Recipe: 100 g water, 40 g BA, 0.025 g, $NaHCO_3$, [APS] = 1 x 10^{-3} mol.dm^{-3}, 60 °C.

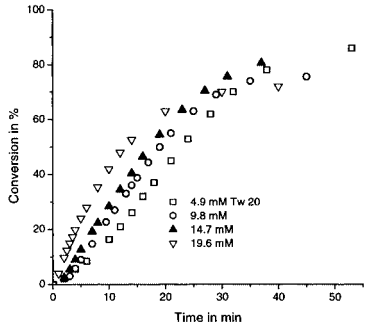

Fig. 5. Variation of monomer conversion with the reaction time and Tw 20 concentration in the (mini)emulsion polymerization of BA initiated by DBP.
Recipe: 100 g water, 40 g BA, 0.025 g $NaHCO_3$, [DBP] = 1 x 10^{-3} mol.dm^{-3}, 60 °C.

The conversion curves have a shape typical for the emulsion polymerization carried out under the nonstationary-state conditions (microemulsion, miniemulsion, or precipitated

polymerization). The final conversions were lower in the classical emulsion polymerisation (CEP) than in the homogenized monomer/Tw 20/water emulsion ((mini)emulsion) polymerization (Table 2). Furthermore, in the CEP the coagulum was inversely proportional

Table 2. Variation of kinetic and colloidal parameters of emulsion and (mini)emulsion polymerization of BA with Tw 20 concentration.[a)]

[Tw 20].10^2 (mol.dm^{-3})		$R_{p,max}$. 10^4 (mol.dm^{-3}.s^{-1})		D (nm)		$N_p.10^{-16}$ /dm^3		Con.$_{fin}$ (%)		Coagulum (wt.%)	
Initiator		1)	2)	1)	2)	1)	2)	1)	2)	1)	2)
APS	0.49	3.0	15	500	330	0.2	1.7	58	86	30	Traces
APS	0.98	4.4	-	300	-	1.5	-	59		25	-
APS	1.96	10.5	18	170	225	7.8	5.4	63	88	10	0
DBP	0.49	-	15	170	311	1.8	2.0	18	87	b)	Traces
DBP	0.98	4.6	15	280	276	1.4	2.5	55	76	25	0
DBP	1.47	10.5	15	180	260	6.9	3.0	67	76	16	0

a) Recipe: 100 g water, 40 g BA, 0.023 g $NaHCO_3$, 60 °C, [DBP] = [APS] = 1 x 10^{-3} mol.dm^3; 1) 400 rpm, 20 min, 2) 25 000 rpm, 10 min, D_w/D_n = 1.3 (emulsion); D_w/D_n = 1.05-1.15 ((mini)emulsion).

to the Tw 20 concentration (especially with DBP). This is not the case with the (mini)emulsion polymerization. The homogenisation, thus, depressed the limited particle agglomeration. This is connected with an increased accumulation of emulsifier within the interfacial layer and it participation on particle stabilization. On the contrary, the location of emulsifier in the monomer droplets (CE) decreases the amount of emulsifier available for the stabilization. This favours the particle flocculation and further immobilization of emulsifier within the particle agglomerates due to which the slow polymerisation occurs at high conversion.

Variations of the rate of polymerization with Tw 20 concentration, the initiator type and conversion are illustrated in Figs. 6 and 7 and Table 3. The three rate intervals (with a distinct Interval 2) typical for the emulsion polymerization do not appear. The profiles of non-stationary rate intervals are more pronounced [39,40]. Interval 2 is overlapped with an abrupt increase of polymerisation rate at low and/or high conversion. First the rate of polymerization (R_p) abruptly increases to the first maximum ($R_{p,max1}$), then decreases to the minimal $R_{p,min}$ or levels off to the constant value (a secondary maximum - the rate shoulder), and finally decreases towards the end of polymerization. The shape of some curves reminds the four rate intervals typical for the miniemulsion polymerization of St [41]. The first maximal

rate (at ca. 20% conversion) was attributed to the formation and growth of polymer particles and the second maximal rate (at ca. 60-70% conversion) to the gel effect. The two maximal rates were also observed in the emulsion polymerization of styrene stabilized by NP40 with the prolonged pre-emulsifier period [25]. The first and second maximal rates (Figs. 6 and 7) were, however, shifted to much lower conversion than those in the classical miniemulsion polymerization of St [41] and emulsion polymerization of St stabilized by NP40 [25]. The first maximal rate is located at ca. 10% conversion, and the second one (a rate shoulder) appears at ca. 40% conversion. The rate of blank polymerization of BA (Recipe: 100 g water, 40 g BA, 0.025 g, $NaHCO_3$, [Tw 20] = 16 mM, 60 °C, without APS) reached the maximum at ca 5% conversion and then continuously decreased with conversion:

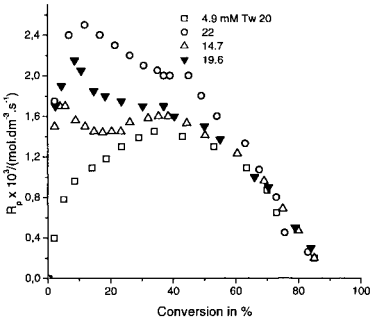

Fig. 6. Variation of the rate of polymerization with conversion and Tw 20 concentration in the (mini)emulsion polymerization of BA initiated by APS. Other conditions see in the legend to Fig. 4.

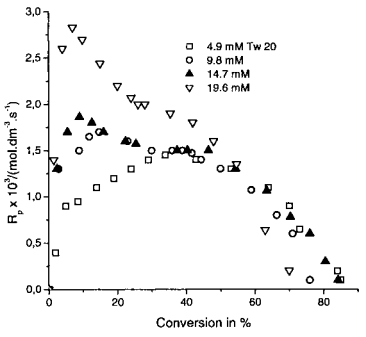

Fig. 7. Variation of the rate of polymerization in the (mini)emulsion polymerization of BA initiated by DBP with conversion and Tween 20 concentration. Other conditions see in the legend to Fig. 5.

$\{R_p \times 10^4/(mol.dm^{-3}.s^{-1})\}/\{Conv./(\%)\}$: 5.9/5, 5.7/10, 5.4/20, 4.5/40, 2.5/60, 0.1/80

The rate of blank polymerization is ca. by one order in magnitude smaller than the rate of polymerization initiated by APS (Fig. 1 and Table 3). The abrupt initial increase in R_p

($R_{p,max,1}$) can partly be attributed to Tw 20 ($Tw_{peroxid}$ 20 formed by the interaction between Tw 20 and oxygen or APS) containing peroxide groups.

According to the micellar model, the reaction order x from the relationship $R_{p,max} \propto [Emulsifier]^x$ is 0.6 [42]. Figs. 6 and 7 and Table 3 show that $R_{p,max,1}$ rises much stronger than $R_{p,max,2}$ with emulsifier concentration. The reaction order x is 0.57 with APS and 0.78 with

Table 3. Variation of kinetic and colloidal parameters of (mini)emulsion polymerization of BA with Tw 20 concentration.[a)]

[Tw 20].10^2 (mol.dm^{-3})	$R_{p,max}$. 10^3 (mol.dm^{-3}.s^{-1})		D (nm)		$N_p.10^{16}$ /dm^3	N_p/N_{drop} [b)]	Con.$_{fin}$ (%)	γ (mN m^{-1})	
	1)	2)	3)	4)	3)			5)	6)
0.49 [c)]	1.0	1.5	330	450 ± 50	1.7	1.8 ± 0.6	86	35	55
1.47 [c)]	1.7	1.6	320	430 ± 50	1.8	1.2± 0.4	87	32	47
1.96 [c)]	2.1	1.8	225	400 ± 50	5.4	4.1±1.4	88	31	47
2.2 [c)]	2.5	2.0	210	380 ± 50	6.4	4.2± 1.6	86	30	46
0.49 [d)]	0.9	1.5	311	450 ± 50	2.0	2.1 ± 0.7	87	35	54
0.98 [d)]	1.7	1.5	276	430 ± 50	2.5	2.4± 0.7	76	33	51
1.47 [d)]	1.9	1.5	260	430 ± 50	3.0	2.8±0.9	76	32	46
1.96 [d)]	2.8	2.0	200	400 ± 50	6.3	4.7±1.6	72	31	44

a) 100 g water, 40 g BA (= 3.1 mol.dm^{-3}), 60 °C, [DBP] = [APS] = 1 x 10^{-3} mol.dm^{-3}, D_w/D_n = 1.05–1.15; b) The ratio of the final number of polymer particles to the initial number of monomer droplets, c) APS, d) DBP, 1) $R_{p,max1}$ 2) $R_{p,max2}$, 3) Final size and number of polymer particles, 4) Initial size of monomer droplets – extrapolated to zero aging time, 5) Surface tension of monomer emulsion, 6) Surface tension of final polymer latex.

DBP (for $R_{p,max,1}$), respectively. The slight deviation from the micellar model favours the effect of $Tw_{peroxid}$ 20. The trend of second maximal rates (the constant rate or the rate shoulder), however, somewhat disfavours the effect of $Tw_{peroxid}$ 20. The slight dependence of $R_{p,max2}$ on [Tw 20] (the reaction order x = 0.19 (for APS) or 0.14 (for DBP)) could result from the accumulation of bound $Tw_{peroxid}$ 20 moieties at particle surface which depress the entry rate of radicals into the particles with fixed interfacial layer. The entry and exit rate coefficients in a polystyrene latex stabilized by poly(oxyethylene)- nonylphenol type emulsifier were an order of magnitude smaller than those for electrostatic - stabilized particles of the same size [44,45]. The thick interfacial layer increases the residence time of radicals within the "hairy" layer which can favor pseudo-bulk kinetics and the gel effect as well. The onset of gel effect in the bulk polymerization of alkyl (meth)acrylate appears at ca. 30% conversion [46]. The gel effect is known to depress the variation of the polymerisation rate with increasing concentration of the reactants. Furthermore, the small reaction order (ca. 0.2) was

observed in the miniemulsion polymerization of MMA stabibilized by SDS/PMMA [43]. According this approach the depressed diffusion of monomer and emulsifier from the monomer droplets to the reaction loci could decrease the reaction order x (diffusion controlled regime).

Activation energy

The overall activation energy (E_o) of emulsion polymerization ($R_{p,emul}$) and solution ($R_{p,sol}$) can be expressed as follows [42,47]:

$$E_{o,emul} = 0.6\ E_p + 0.4\ E_d \quad (1)$$

$$E_{o,sol} = E_p - 0.5\ E_t + 0.5\ E_d \quad (2)$$

where E_p is the activation energy for propagation, E_t is the activation energy for termination, and E_d is the activation energy for decomposition of initiator. For most monomers, E_p , E_t , and E_d are 30, 20, and 125 kJ mol^{-1}, respectively [48]. Using eqs. 1 and 2, the overall activation energy is estimated to be ca. 90 kJ mol^{-1} for solution or bulk polymerization and ca. 70 kJ mol^{-1} for emulsion polymerization, respectively. $R_{p,max}$ data (at 10 and 40% conversion) obtained from Figs. 8 and 9 were used to get the Arrhenius plot (ln $R_{p,max}$ vs. 1/T) and the overall activation energy ($E_{o,emul}$) as well (Fig. 10). The estimated $E_{o,APS,10\%\ conv}$ = 40.6 $kJ.mol^{-1}$, $E_{o,APS,40\%\ conv}$ = 54.4 $kJ.mol^{-1}$, $E_{o,DBP,\ 10\%\ conv.}$ = 18.2 $kJ.mol^{-1}$ and $E_{o,DBP,\ 40\%\ conv.}$ = 25.4 $kJ.mol^{-1}$ are much smaller than those estimated from Eqs. 1 and 2. These values are also smaller than those (48 $kJ.mol^{-1}$ and 56.6 $kJ.mol^{-1}$ estimated from the maximal rate) obtained in the emulsion polymerisation of St stabilized by Tw 20 and initiated by APS and DBP, respectively [49]. The overall activation energy ($E_{o,emul}$) for the miniemulsion polymerization of

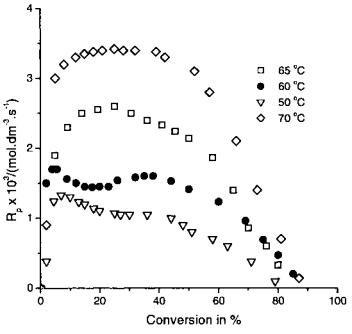

Fig. 8. Variation of the rate of polymerization in the (mini)emulsion polymerization of BA initiated by APS with temperature. Recipe: 100 g water, 40 g BA, 0.025 g $NaHCO_3$, [APS] = 1 x 10^{-3} $mol.dm^{-3}$, [Tw 20] = 1.47 x 10^{-2} $mol.dm^{-3}$.

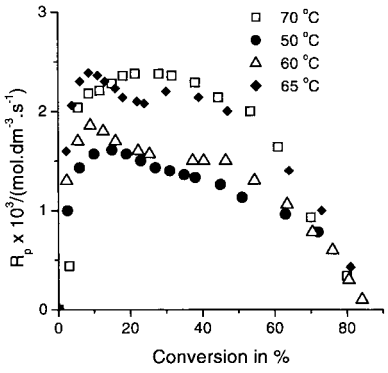

Fig. 9. Variation of the rate of polymerization in the (mini)emulsion polymerization of BA initiated by DBP with temperature. Recipe: 100 g water, 40 g BA, 0.025 g $NaHCO_3$, [DBP] = 1 x 10^{-3} mol.dm^{-3}, [Tw 20] = 1.47 x 10^{-2} mol.dm^{-3}.

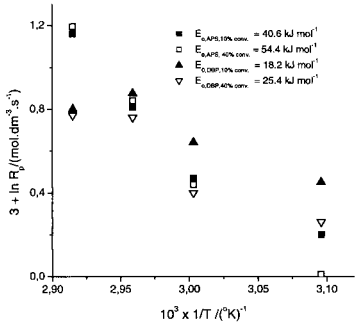

Fig. 10. The Arrhenius plot (the polymerization rate vs. 1/T) for the (mini)emulsion polymerization of BA initiated by APS or DBP. Other conditions see in the legend to Figs. 8 and 9.

styrene stabilized by SDS and initiated by peroxodisulfate was reported to be 61.5 kJ mol^{-1} [50]. The low $E_{o,emul}$ = 34.3 kJ mol^{-1} was estimated from the initial rates of microemulsion polymerization of styrene (50 °C - 80 °C) [51]. According to Eq. 1 $E_{o,emul}$ is governed by two terms the decomposition of initiator (the initiation (E_d)) and the monomer propagation. The increased barrier for radicals entering the polymer particles was suggested to increase $E_{o,emul}$ [52]. The reverse behavior is expected for the sterically stabilized polymer particles. The barrier for entering radicals resulting from the thick interfacial surface layer decreases with increasing temperature. For example, the effective thickness of the adsorbed layer of nonionic emulsifier octaoxyethylene glycol n-dodecyl monoether on PSt polymer particle decreased with increasing temperature from a value 6.2 nm at 15 °C to 2.2 nm at 43 °C [53]. The low $E_{o,emul}$ can be attributed to decreased barrier for entering radicals into the polymer particles

with increasing temperature. The barrier for radicals entering the polymer particles is more pronounced for the charged oligomeric radicals (derived from APS) than for noncharged (derived from DBP) ones (Fig. 10).

The effect of initiating radical located within the interfacial layer was studied with the $Tw_{peroxid}$ 20. The rate of blank emulsion polymerization of BA varies with temperature as follows:

$$\{R_{p,max1} \times 10^4/(mol.dm^{-3}.s^{-1})\}/\{Temp./(^{\circ}C)\}: 4.3/30, 4.9/50, 5.9/60, 7.2/70$$

The activation energy for the blank polymerization was estimated to be ca. 11 kJ mol^{-1}. The small activation energy results from the low barrier for $Tw_{peroxid}$ 20 entering the polymer particles. The location of $Tw_{peroxid}$ 20 at the particle surface and/or in the monomer (dissolved Tw 20) droplets strongly decreases the activation energy of initiation. The further decrease in E_d results from the decrease of thickness of the adsorbed layer of Tw 20 at particle surface with increasing temperature. The difference between $E_{o,emul,\ 10\%\ conv.}$ and $E_{o,emul,\ 40\%\ conv.}$ results from the increased barrier for entering radicals caused by accumulation of chemically bound emulsifier moieties at the particle surface.

Colloidal parameters

The average hydrodynamic particle size increases with conversion for both APS and DBP initiated (mini)emulsion polymerisation of BA (Fig. 11). The polymer particles were larger with APS than with DBP. The reversed behaviour was observed in the emulsion or microemulsion polymerization of BA or St where the polymer particles were always larger in the polymerization systems initiated with an oil-soluble initiator than with a water-soluble initiator [18,39,54]. In the microemulsion system the particle size slightly increased with conversion [39,55]. In the classical emulsion system stabilized by nonionic emulsifier, the particle size increased with increasing conversion and the increase was much more pronounced at low conversion [4,56].

Fig. 12 shows that the particle number (N_p) increases with emulsifier concentration and conversion up to ca. 40% and then reaches a plateau. The oil-soluble initiator (DBP) produces larger number of particles than the water soluble one (APS) (see also Tables 2 and 3). The low water solubility of DBP means that the fraction of initiating radicals formed by decomposition of DBP in the aqueous phase is negligible. This can be a reason why the

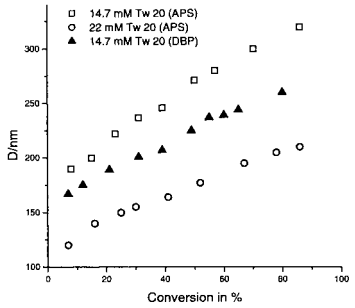

Fig. 11. Variation of the average particle diameter (D) in the (mini) emulsion polymerization of BA with Tw 20 concentration, type of initiator and conversion. Recipe: 100 g water, 40 g BA, 0.025 g $NaHCO_3$, [DBP] = [APS] = 1 x 10^{-3} $mol.dm^{-3}$, 60 °C.

increased formation of radicals within the monomer-swollen micelles or monomer droplets by the decomposition of DBP increased the particle nucleation. The particle nucleation is also favoured by the lower barrier for radicals derived from DBP radicals entering the sterically stabilized monomer-swollen micelles. In the microemulsion polymerization the number of particles increases with a constant rate up to the final conversion [39,55]. In the miniemulsion polymerization N_p increases up to ca. 40 - 50% conversion.[13,40,41]. The increase in N_p results from the continuous release of emulsifier from the monomer droplets (degradation of

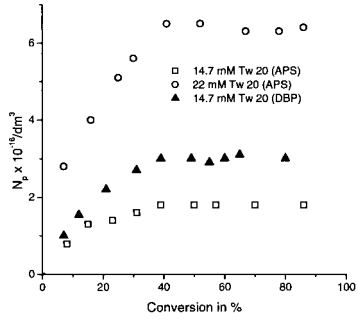

Fig. 12. Variation of the particle number (N_p) in the (mini)emulsion polymerization of BA with Tw 20 concentration, type of initiator and conversion. Other conditions see in the legend to Fig. 9.

emulsifier saturated monomer droplets) and the contribution of monomer droplets (Table 3). The ratio of the final number of polymer particles to the initial number of monomer droplets (N_p/N_{drop}) varies from 1.2 to 4.7 which is in favour of the partial monomer droplet nucleation.

The apparent particle size distribution (PSD = D_w/D_n) of polymer latexes of coarse Tw 20/BA emulsions was ca. 1.3. More uniform polymer latexes were prepared by polymerization of BA/Tw 20 (mini)emulsions (PSD ca. 1.05-1.15) (Tables 2 and 3). In the former case, the polymerization was accompanied with a large amount of coagulum and the final conversion ca. 20 – 40wt%. The (mini)emulsion polymerisation stabilized with [Tw 20]

$\geq$ 0.015 mol.dm^{-3} generated polymer latexes without coagulum. The small amount of coagulum (< 1 wt%) appeared in the (mini)emulsion containing the smallest amount of [Tw 20] = 4.9 mM. In the non-homogenized emulsions the presence of large droplets or particles is accompanied with the particle flocculation or coagulation [57]. The very large monomer/polymer polymer particles (ca 1 000 nm) were observed at the beginning of CE polymerization (ca. 1 000 nm). This was not true in the (mini)emulsion polymerisation containing more uniform monomer droplets. The high oil solubility of Tw 20 decreases the amount of emulsifier available for stabilization. This can be somewhat depressed by the homogenisation of monomer emulsion which increases the interface area and the location of larger fraction of emulsifier in the interface layer [40,58].

The reaction orders x_{Tw} = 0.8 (APS) and 0.74 (DBP) obtained from the dependence $N_p \propto$ [emulsifier]^x (Table 3) deviate from the micellar model [42]:

$$N_p \propto [E]^{0.6} [I]^{0.4} \qquad (3)$$

The increase in the reaction order x_{Emul} is attributed to the limited particle flocculation operative at low emulsifier concentration. The presence of a small amount of $Tw_{peroxid}$ 20 can also increase the reaction order x_{Tw}. The latter can explains the strong deviation of the

Table 4. Variation of kinetic and colloidal parameters of pseudo-miniemulsion polymerization of BA with initiator concentration.[a]

[Initiator].10^2 Type (mol.dm^{-3})		$R_{p,max1}$ $R_{p,max2}$. 10^3 (mol.dm^{-3}.s^{-1})		D (nm)	$N_p.10^{16}$ /dm^3	Conv.$_{fin}$ (%)	γ [b] (mN.m^{-1})
APS	1.0	2.6	2.3	260	3.5	87	48
APS	0.5	2.3	2.7	291	2.6	94	
APS	0.28	1.9	2.0	320	1.8	86	50
APS	0.1	1.7	1.6	320	1.8	87	47.4
DBP	1.0	2.5	2.2	260	3.2	79	46.3
DBP	0.3	1.9	1.6	255	3.2	75	46.5
DBP	0.1	1.9	1.5	260	3.0	76	46
DBP	0.05	1.7	1.4	267	2.8	76	44.3

a) 100 g water, 40 g BA, Polym. temp. 60 °C, [Tween 20] = 1.47 x 10^{-2} mol.dm^{-3}, b) Surface tension of final polymer latex at ca. 25 °C, surface tension of monomer emulsion was varied in the range 31-32 mM.m^{-1}.

dependence $N_p \propto$ [Initiator]^x (the reaction order x_{APS} = 0.22 and x_{DBP} = 0.03, data taken Table 4) from the micellar model. The rate of initiation given by the decomposition of APS or DBP can be overlapped by the presence of $Tw_{peroxid}$ 20. The independence of N_p on [DBP] favours the primary radical termination as well. The very low slope of the dependence of the

$R_{p,max1,2}$ vs. [initiator] was also observed for DBP (Table 4). The charged (surface active) radicals derived from APS can take part in the homogeneous nucleation and so increase the particle nucleation rate (x_{APS} = 0.22). The lower slope of the (line) dependence ($N_p \propto$ [initiator]^x, x_{KPS} = 0.11) was reported for the classical miniemulsion polymerization of MMA initiated by peroxodisulfate initiator where the monomer droplet nucleation was dominant [59]. This was believed to correspond to the point in which all droplets become nucleated. In the classical miniemulsion polymerization the final particle number is the same as the initial droplet number. The ratio of the final number of polymer particles to the initial number of monomer droplets ($N_p/N_{drop} > 1$) supports the limited monomer droplet nucleation in the (mini)emulsion polymerization of BA (Table 3).

Conclusion

The clouding temperature of the aqueous Tween 20 (Tw 20) solution was estimated to be ca. 80 °C and it was nearly independent of emulsifier concentration. The cloud point of Tw 20 abruptly decreased by the addition of a small amount of monomer. The clouding temperature of the ternary monomer/Tw 20/water system increased with increasing emulsifier concentration and the increase was more pronounced with butyl acrylate (BA) than with styrene (St). The rate of (mini)emulsion (homogenized emulsion) polymerization vs. conversion curve shows the non-stationary rate intervals. The onset of interval 2 is overlapped with the fast polymerisation at low and high conversion. The first maximal rate ($R_{p,max,1}$) is attributed to the increased number of polymer particles, the monomer-saturated condition and the presence of a small amount of Tw 20 containing peroxide groups ($Tw_{peroxid}$ 20). The second maximal rate or plateau ($R_{p,max,2}$) is attributed to the end of stationary-rate interval. The followed decreased rate of polymerization results from the depressed transfer of monomer from the droplets to the reaction loci. $R_{p,max,1}$ rises much stronger than $R_{p,max,2}$ with emulsifier concentration. This was discussed in terms of the increased contribution of $Tw_{peroxid}$ 20 at low conversion and increased contribution monomer-starved condition at high conversion. The slight dependence of $R_{p,max,1}$ and $R_{p,max,2}$ on the initiator concentration supports the contribution of $Tw_{peroxid}$ 20 and the gel effect at high conversion. The low apparent activation energy was ascribed to the decreased barrier for radicals entering into the polymer particles with increasing temperature. The very low activation energy for blank polymerization (initiated by $Tw_{peroxid}$ 20) results from the location of initiating radicals (derived from $Tw_{peroxid}$ 20) at the particle surface or in the monomer/polymer particles. The

contribution of blank polymerization decreases the overall activation energy for the emulsion polymerization of BA initiated by APS or DBP. The ratio of the final number of polymer particles to the initial number of monomer droplets (N_p/N_{drop}) promotes the partial monomer droplet nucleation. The dye method demonstrated the presence of monomer droplets at high conversion for both the (mini)emulsion polymerization and the polymerization with the prolonged-emulsification time. The foregoing results indicate that the polymerization rate is a complex function of following effects: 1) the increased number of particles and the decreased monomer concentration at reaction loci with conversion, 2) the increased stability of monomer droplets, 3) the continuous release of emulsifier from monomer droplets, 4) the contribution of $Tw_{peroxid}$ 20, 5) the gel effect, etc.

Acknowledgement: This work was supported by the Slovak Grant Agency VEGA through the grant number 2/1014/21.

References

1. D. J. Mitchell, G. Tiddy, L. Waring, T. Bostock, I. P. Mc Donald, J. Chem. Soc., Faraday Trans. 1, **79**, 975 (1983)
2. R. Kjellander, J .Chem. Soc., Faraday Trans. 2, **78**, 2025 (1982)
3. H. Schott, J. Colloid Interface Sci. **43**, 150 (1973)
4. K. Weckstrom, M. Zulauf, J. Chem. Soc., Faraday Trans. **81**, 2947 (1982)
5. G. Briganti, S. Puvada, D. Blankschtein, J. Phys. Chem. **95**, 8989 (1991)
6. Y. Tokuoka, H. Uchiyama, M. Abe, K. Ogino, J. Colloid. Interface Sci. **152**, 402 (1992)
7. D. Blankschtein, G. Thurston, G, Benedek, J. Chem. Phys. **84**, 4558 (1986); ibid. **86**, 7268 (1986)
8. F. Testard, Th. Zemb, Langmuir **14**, 3175 (1998)
9. C. B. Dittman-McBain, I. Piirma, J. Appl. Polym. Sci. **37**, 1415 (1989)
10. S. M. Mahdi, R. O. Skold, Colloids and Surfaces **66**, 203 (1992)
11. W. Ostwald, Phys. Chem. **37**, 385 (1901)
12. C. M. Miller, E. D. Sudol, C. A. Silebi, M. S. El-Aaasser, Macromolecules **28**, 2754, 2765, 2772 (1995)
13. J. Rubio, J. A. Kitchener, J. Colloid Interface Sci. **57**, 132 (1976)
14. J. A. De Witt, T. G. M. van de Ven, Adv. Colloid Interface Sci. **42**, 41 (1992)
15. Z. Haq, L. Thomson, Colloid Polym. Sci. 260, 212 (1982)
16. M. J. Rosen, Surfactants and Interfacial Phenomena. John Wiley, New York, p. 119, 1988
17. I. Capek, Makromol. Chem. **190**, 789 (1989)
18. P. Potisk, I. Capek, Angew. Makromol. Chemie **222,** 125 (1994)
19. I. Capek, P. Potisk, Eur. Polym. J. **31**, 1269 (1995)
20. J. Reimers, F. J. Schork, J. Appl. Polym. Sci. **60**, 251 (1996)
21. W. D. Harkins, J. Am. Chem. Soc. **69**, 1428 (1947)
22. K. Toerne, R. Rogers, R. von Wandruszka, Langmuir **16**, 2141 (2000)
23. D. J. Mitchell, G. Tiddy, L. Waring, T. Bostock, I. P. Mc Donald, J. Chem. Soc., Faraday Trans. 1, **79**, 975 (1983)

24. P. H. Elworthy, C. McDonald, Kolloid-Z **16**, 195 (1964)
25. S. Y. Lin, I. Capek, T. J. Hsu, C. S. Chern, J. Polym. Sci. Polym. Chem. **37**, 4422 (1999)
26. J. Weiss, D. J. McClements, Langmuir **16**, 5879 (2000)
27. K. Shinoda, H. Takeda, J. Colloid Interface Sci. 32, 642 (1970)
28. D.Blankschtein, G.Thurston, G,Benedek, J.Chem. Phys. 85, 7268 (1986), ibid. 84, 4558 (1986)
29. I. Capek, C.W.Liou, C.S. Chern, J. Chin. Inst. Chem. Engn., Vol. 32, 327 (2001)
30. M. J. Jaycock, G. D. Parfitt, Chemistry of Interfaces, Ellis Horwood, New York 1980
31. R. J. Hunter, Foundations of Colloid Science; Clarendon Press: Oxford, Vol. 1, p. 233 (1986)
32. B. R. Vijayendran, J. Appl. Polym. Sci., **23**, 733 (1979)
33. K. Kamogawa, M. Matsumoto, T. Kobayashi, T. Sakai, H. Sakai, M. Abe, Langmuir **15**, 1913 (1999)
34. G. L. Gaines, J. Polym. Sci. A2, **7**, 1379 (1969)
35. J. L. Gordon, J. Polym. Sci. **6**, 623, 643, 665, 687 (1968)
36. C. S. Chern, Y. C. Liou, Macromol. Chem. Phys. **199**, 2051 (1998)
37. C. S. Chern, T. J. Chen, Y. C. Liou, Polymer **39**, 3767 (1998)
38. S. Y. Lin, I. Capek, T. J. Hsu, C. S. Chern, Polym. J. **32**, 932 (2000)
39. I. Capek, Adv. Colloid Interface Sci. **80**, 85 (1999); ibid. **82**, 253 (1999)
40. I. Capek, C. S. Chern, Adv. Polym. Sci. **155**, 101 (2001)
41. C. M. Miller, E. D. Sudol, C. A. Silebi, M. S. El-Aasser, J. Polym. Sci. Polym. Chem. Ed **33**, 1391 (1995)
42. W. V. Smith, R. H. Ewart, J. Am. Chem. Soc. **70**, 3695 (1948)
43. J. Reimers, F. J. Schork, J. Appl. Polym. Sci. **59**, 1833 (1996)
44. E. Coen, R. A. Lyons, R. G. Gilbert, Macromolecules **29**, 5128 (**1996**)
45. J. M. H. Kusters, D. H. Napper, R. G. Gilbert, A. L. German, Macromolecules **25**, 7043 (1992)
46. J. Dionisio, H. K. Mahabadi, K. F. O'Driscoll, J. Polym. Sci., Polym. Chem. Ed. **17**, 1891 (1979)
47. G. Odian, Principles of polymerization, 2nd ed., Wiley, New York, 1981
48. J. Brandrup, E. H. Immergut, Polymer Handbook, 3rd Edn. John Wiley and Sons, New York, 1989
49. J. Chudej, I. Capek, J. Polym. Sci., in press
50. Y. Y. Choi, Ph.D dissertation, Lehigh University, Bethlehem, PA, 1986
51. L. Feng, K. Y. S. Ng, Macromolecules, **23**, 1048 (1990)
52. L. M. Gan, C. H. Chew, J. H. Lim, K. C. Lee, L. H. Gan, Colloid Polym. Sci. 272 1089 (1994)
53. L. Thomson, D. N. Pryde, J. Chem. Soc., Faraday Trans. 1, 77, 2405 (1981)
54. I. Capek, J. Barton, A. Karpatyova, Makromol.Chem. **188**, 703 (1987)
55. J. S. Guo, M. S. El-Aasser, J. W. Vanderhoff, J. Polym. Sci. Polym. Chem. **30**, 691, 703 (1992)
56. I. Capek, M. Mlynarova, J. Barton, Makromol. Chem. **189**, 341 (1988)
57. J. Th. G. Overbeek, in Colloid Science, H. R. Kruyt, Ed., Elsevier, Amsterdam, Vol.2, p.290 (1952)
58. P. J. Blythe, A. Klein, E. D. Sudol, M. S. El-Aasser, Macromolecules **32**, 4225, 6944, 6952 (1999)
59. K. Fontenot, F. J. Schork, J. Appl. Polym. Sci. **49**, 633 (1993)